Mem. S.A.It. Vol. 83, 482

Memorie della

Supersoft x-ray phases of mass-accreting white dwarfs

I. Hachisu

Department of Earth Science and Astronomy, College of Arts and Sciences, University of Tokyo, Komaba 3-8-1, Meguro-ku, Tokyo 153-8902, Japan
e-mail: hachisu@ea.c.u-tokyo.ac.jp

Abstract. I review various supersoft X-ray phases of mass-accreting (WDs). Response of WDs to the mass accretion from the companion is divided into three cases: (1) optically thick winds blow when the mass accretion rate to the WD exceeds a critical rate, $\dot{M}_{\rm acc} > \dot{M}_{\rm cr}$, and the WD mass is steadily increasing with a relatively high rate of $\dot{M}_{\rm cr}$, (2) supersoft X-ray phases are observed for a narrow range of mass-accretion rates of $\dot{M}_{\rm st} < \dot{M}_{\rm acc} < \dot{M}_{\rm cr}$, i.e., hydrogen shell-burning without optically thick winds, (3) intermittent shell flashes occur for lower mass-accretion rates of $\dot{M}_{\rm acc} < \dot{M}_{\rm st}$. First, as examples of the wind case, I present a self-sustained model for long-term light-curve variations of the supersoft X-ray sources, RX J0513.9−6951 and V Sge. Second, based on a universal decline law of classical novae, I describe a theoretical duration of supersoft X-ray phase of classical novae and compare them with observation. I also introduce the absolute magnitude of our free-free emission model light curves, and derived theoretical maximum magnitude versus rate of decline (MMRD) relations.

Key words. Novae, cataclysmic variables – Stars: individual (RX J0513.9−6951, V Sge) – Stars: mass loss – White dwarfs – X-rays: stars

1. Introduction

Supersoft X-ray sources (SSSs) are hydrogen shell-burning white dwarfs (WDs) in binary systems. Figure 1 plots positions of several SSSs in the HR diagram, indicating that the positions are just coincident with loci of hydrogen shell-burning WDs with various masses. There are theoretically three cases of the response of WDs to the mass accretion rate from the companion: (1) mass-accreting WDs blow optically thick winds when the mass accretion rate to the WD exceeds a critical rate, i.e., $\dot{M}_{\rm acc} > \dot{M}_{\rm cr} \sim 1 \times 10^{-6} M_\odot$ yr^{-1} (Hachisu et al. 1996; Kato & Hachisu 1994). Hydrogen shell-burning is stable and the WD mass is increasing with a relatively high rate of $\dot{M}_{\rm cr}$. We do not observe supersoft X-rays because the photospheric temperature is relatively low and super soft X-rays are self-absorbed by the wind itself. (2) Only in a narrow range of the mass-accretion rates of $\dot{M}_{\rm st} < \dot{M}_{\rm acc} < \dot{M}_{\rm cr}$, we have steady SSSs. Hydrogen shell-burning is stable and the WD mass is increasing with a rate of $\dot{M}_{\rm acc}$. See Figure 2 for this narrow strip in the WD mass versus mass-accretion rate diagram. (3) Hydrogen shell-burning is unstable to trigger a shell flash on the WD when $\dot{M}_{\rm acc} < \dot{M}_{\rm st}$ and they are observed as novae or recurrent novae. These WDs become a SSS only in a later phase of the shell flashes.

Send offprint requests to: Izumi Hachisu

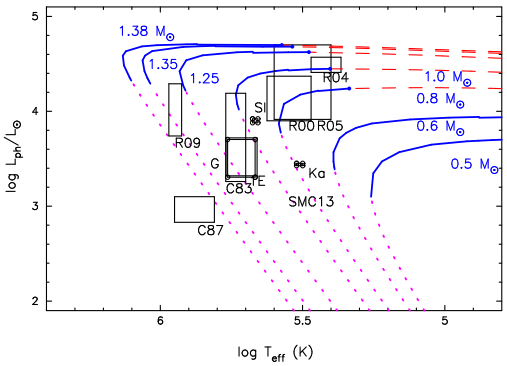

Fig. 1. Positions of several supersoft X-ray sources and loci of hydrogen shell-burning WD models in the H-R diagram (taken from Nomoto et al. 2007). The WD mass is attached to each curve. The solid and dashed line-parts denote stable hydrogen shell-burning, while the dotted line parts correspond to unstable burning (nova WDs in a later phase and in quiescence). In the dashed line parts, the optically thick winds are predicted to blow (Kato & Hachisu 1994), so that supersoft X-rays could be absorbed by the wind itself and not be detected. Positions of several supersoft X-ray sources are plotted by squares, i.e., R09 (RX J0925.7−4758), C87 (CAL87), C83 (CAL83), 1E (1E0035.4−7230), R00 (RX J0019.8+2156), R04 (RX J0439.8−6809), R05 (RX J0513.9−6809).

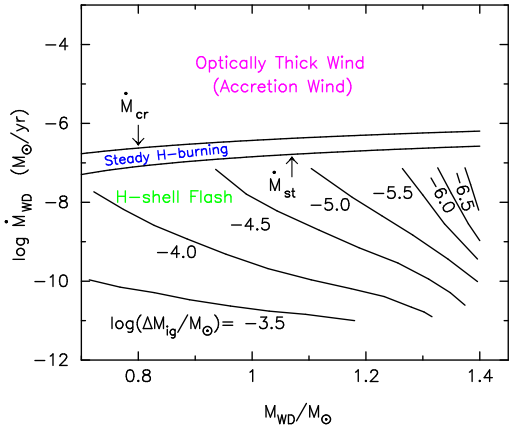

Fig. 2. Response of WDs to mass accretion in the $M_{\rm WD}$-$\dot{M}_{\rm acc}$ plane (taken from Hachisu & Kato 2001). Stable hydrogen shell burning occurs when $\dot{M}_{\rm acc} \geq \dot{M}_{\rm st}$. Strong optically thick winds blow when $\dot{M}_{\rm acc} > \dot{M}_{\rm cr}$. The wind mass loss rate is $\dot{M}_{\rm wind} = \dot{M}_{\rm acc} - \dot{M}_{\rm cr}$ and the WD mass is increasing with a relatively high rate of $\dot{M}_{\rm cr}$. Steady hydrogen shell burning with no optically thick winds occur when $\dot{M}_{\rm st} \leq \dot{M}_{\rm acc} \leq \dot{M}_{\rm cr}$. There are no steady-state burning when $\dot{M}_{\rm acc} < \dot{M}_{\rm st}$. Intermittent shell flashes (novae) occur. The envelope mass, $\Delta M_{\rm ig}$, at which hydrogen shell flash occurs, is also shown (taken from Figure 9 of Nomoto 1982).

2. Binaries with intermittent optically thick winds

Optically thick winds blow from the WD when the mass accretion rate to the WD exceeds a critical rate ($\dot{M}_{\rm cr}$) as shown in Figures 2 and 3. If the wind collides with the companion and strips off its surface, the mass accretion rate to the WD could be suppressed. We show two such examples of SSSs, RX J0513.9−6951 and V Sge. The Large Magellanic Cloud (LMC) transient supersoft X-ray source RX J0513.9−6951 (hereafter RX J0513) was discovered by *ROSAT*. Its remarkable observational features are summarized as follows: (1) Optical monitoring of RX J0513 shows quasi-regular transitions between high ($V \sim 16.6$) and low ($V \sim 17.4$) states (Alcock et al. 1996). (2) The duration of the optical high state is $\sim 60 - 150$ days while the low states last for ~ 40 days (Fig. 4a). (3)

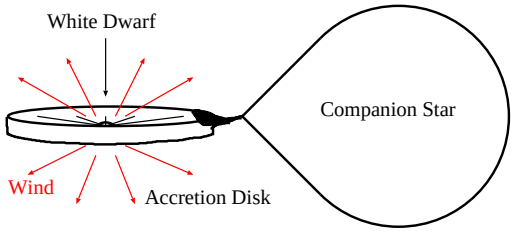

Fig. 3. Optically thick winds blow from the mass-accreting WD (left) when the mass accretion rate from a lobe-filling companion (right) exceeds a critical rate ($\dot{M}_{\rm acc} > \dot{M}_{\rm cr}$). Winds collide with the companion and strip off the surface layer. Stable hydrogen burning on the WD converts hydrogen into helium and, as a result, the WD mass is increasing with a relatively high rate of $\dot{M}_{\rm cr}$.

Copious supersoft X-rays ($\sim 30 - 40$ eV) were detected only in the optical low state (Reinsch et al. 2000). (4) The transitions between X-ray off and on are very rapid, about one day or so, while the optical transitions from high to low

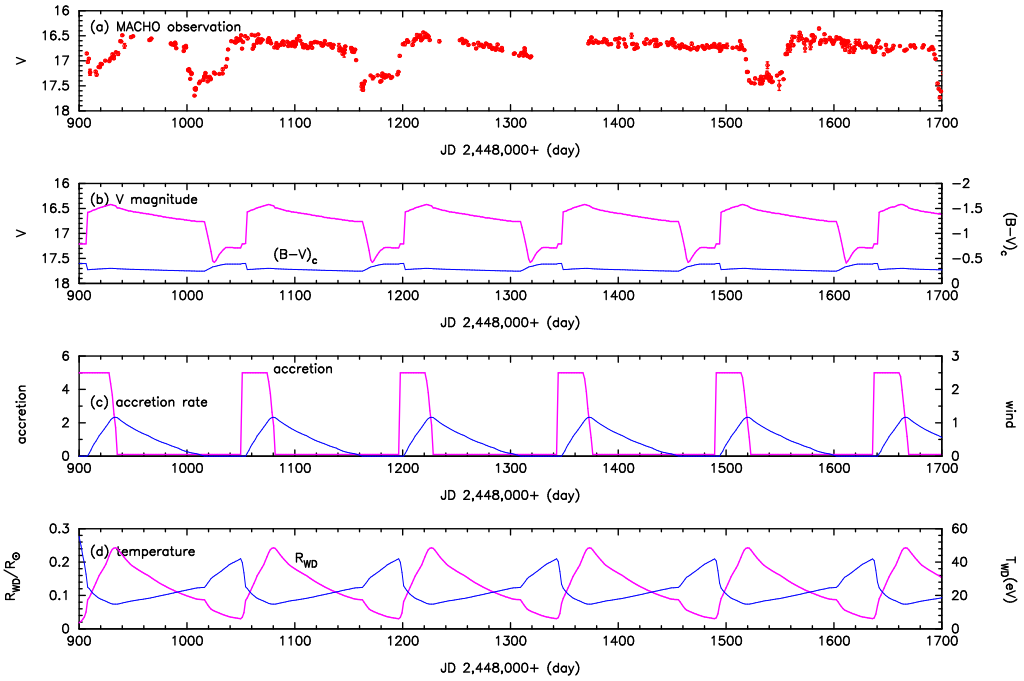

Fig. 4. Numerical results of our RX J0513.9−6951 model taken from Hachisu & Kato (2003a): (a) observational V magnitudes (Alcock et al. 1996); (b) calculated V magnitudes (thick solid line) together with $B-V$ color (thin solid line); (c) mass accretion rate to the WD ($\dot{M}_{\rm acc}$, thick solid line) and wind mass-loss rate from the WD ($\dot{M}_{\rm wind}$, thin solid line), both in units of $10^{-6}M_\odot{\rm yr}^{-1}$; and (d) photospheric radius of the WD envelope in units of $R_\odot$ (thick solid line) and surface temperature of the WD envelope in units of eV (thin solid line). The model parameters are $M_{\rm WD}=1.3\ M_\odot$, $\dot{M}_{\rm MS}=5.0\times10^{-6}M_\odot\ {\rm yr}^{-1}$, $c_1=10.0$, and $t_{\rm vis}=20.5$ days. Direct fitting to the brightness of the observational light curves indicates an apparent distance modulus of $(m-M)_V=18.7$.

occur over several days (e.g., Reinsch et al. 2000).

Long-term variations in the optical light curves of RX J0513 are considered as a limit cycle. We adopt a binary system consisting of a WD, a disk around the WD, and a lobe-filling main-sequence (MS) companion. An essential thing is that WDs blow optically thick, strong winds when $\dot{M}_{\rm acc}>\dot{M}_{\rm cr}\sim1\times10^{-6}M_\odot\ {\rm yr}^{-1}$ (Hachisu et al. 1996) as illustrated in Figure 3. This condition is satisfied if the MS companion is $\sim2-3\ M_\odot$ because the mass-transfer rate from the MS, $\dot{M}_{\rm MS}$, is as large as a few times $10^{-6}M_\odot\ {\rm yr}^{-1}$ or more.

When a rapid mass accretion to the WD begins, the WD envelope expands to blow an optically thick, strong wind. The strong wind causes a quick rise of V magnitude because the disk expands from a few to several times the previous size. Since the irradiated disk is the main source in the optical light, this expansion of the disk area causes a magnitude rise in the optical light. The wind mass loss rate increases from zero to $\dot{M}_{\rm wind}\sim1\times10^{-8}M_\odot\ {\rm yr}^{-1}$ or more in a day, which is massive enough to absorb supersoft X-rays. Thus, this phase is the optical high and X-ray−off state. The strong wind hits the MS companion and then strips off its surface layer. The stripped gas is lost from the binary. Therefore, the rapid mass accretion is suppressed by the strong wind itself. As the wind mass-loss rate increases, the mass-stripping rate eventually overcomes the mass-transfer rate. Then, mass accretion to the WD stops. The mass of the WD envelope is now gradually decreasing, mainly as a result of

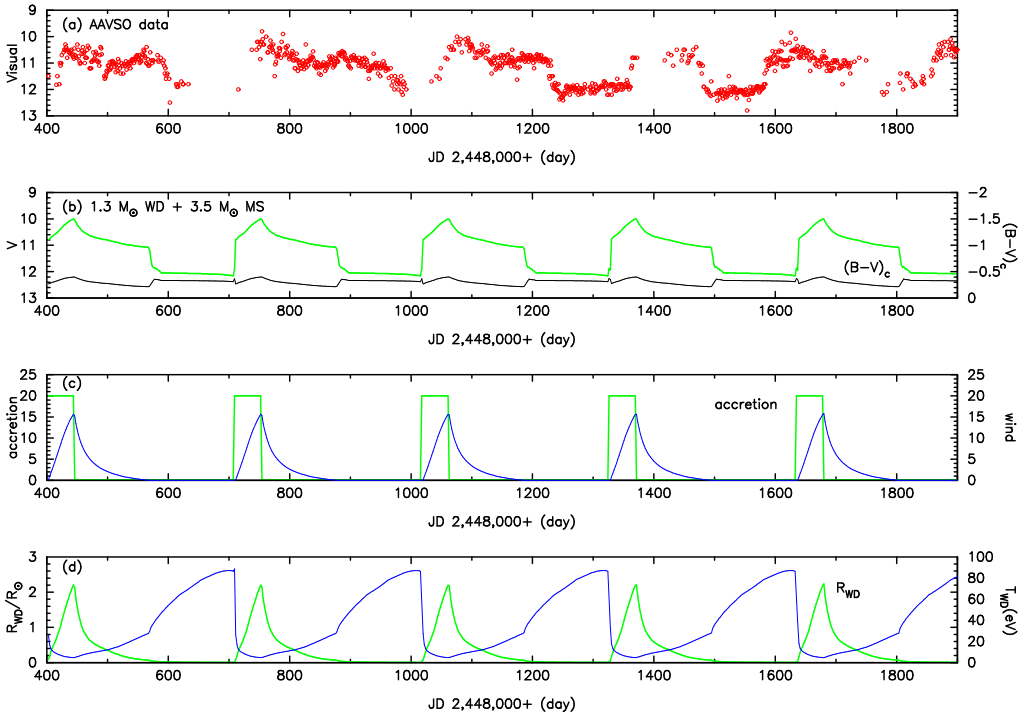

Fig. 5. Same as Fig.4 but for a Galactic SSS V Sge taken from Hachisu & Kato (2003b). (a) One-day means of the out-eclipse AAVSO data of V Sge (Šimon & Mattei 1999) against time (JD 2,448,000+). (b) V-magnitude light curves (thick solid line) of our V Sge model (1.3 $M_\odot$ WD and 3.5 $M_\odot$ MS). The calculated light curves are made by connecting the brightness at orbital phase 0.4. (c) and (d) are the same as those in Fig.4 bur for our V Sge model.

wind mass loss. The photosphere of the WD is also gradually shrinking. This causes a gradual decay of the optical light curve even if the disk shape is the same. The wind eventually stops.

We expect copious supersoft X-rays after the wind stops. The disk shrinks to a normal previous size. This causes a sharp $\sim$ 1 mag drop in the optical light. A rapid mass transfer from the MS to the disk resumes and then the disk edge flares up. This phase corresponds to the optical low and X-ray−on state. Thus, the cycle is repeated. The numerical results are shown in Figure 4. See Hachisu & Kato (2003a) for more details. V Sge in our Galaxy also shows quasi-periodic optical high (soft X-ray−off) and low (soft X-ray−on) states with the total period of $\sim$ 300 days, longer than RX J0513. A binary model similar to RX J0513 is proposed to explain the long term variation of the light curve. The main differences from RX J0513 are that (1) the mass transfer rate from the MS companion in V Sge is much larger than that in RX J0513 as shown in Figure 5 and that (2) the metallicity in V Sge is about three times larger than that in RX J0513 and the wind is stronger.

These make the differences between two objects. See Hachisu & Kato (2003b) for more details. The WDs in RX J0513 and V Sge are now constantly growing in mass at a critical rate of $\dot{M}_{\rm cr}$. We expect that the WD masses increase up to the Chandrasekhar mass and they eventually explodes as a Type Ia supernova.

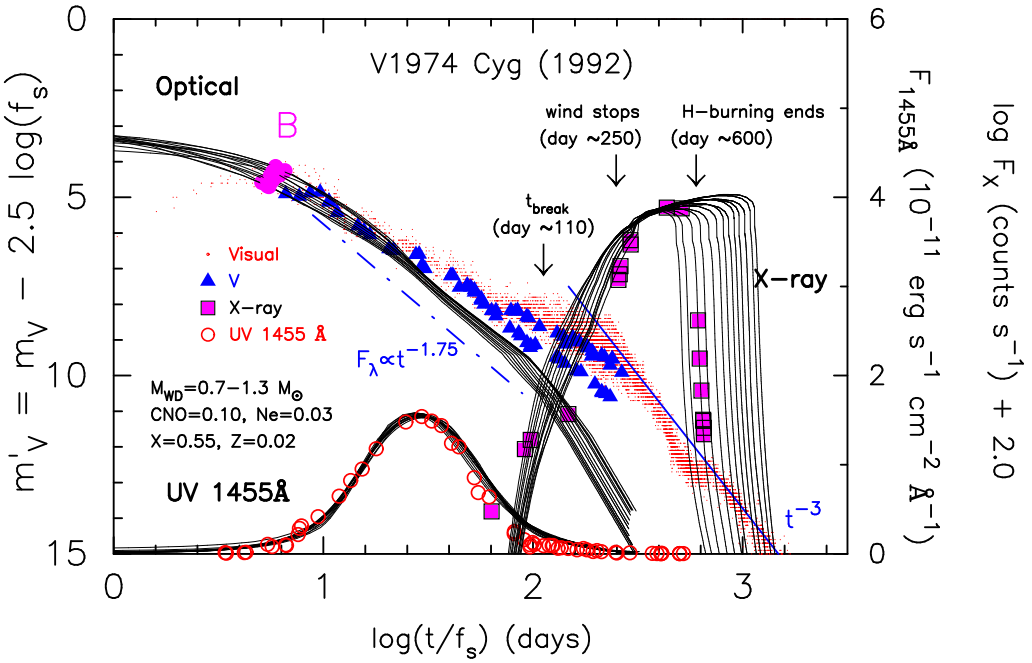

Fig. 6. Nova model light curves squeezed by f_s taken from Hachisu & Kato (2010). Observational data of the neon nova V1974 Cyg is added for comparison. Thirteen different WD mass models (0.7 – 1.3 $M_\odot$ by 0.05 $M_\odot$ step). We squeeze or stretch the model light curve along time to fit with the observational data of V1974 Cyg, i.e., *ROSAT* X-ray observation, optical, and *IUE* UV 1455Å light curves. Here we set point B on each model light curve near t_0 (optical V peak). Here $t_{\rm break}$ corresponds to a break of the model light curve changing from a slope of $t^{-1.75}$ to t^{-3}.

3. Supersoft x-ray phases of classical novae

Classical novae are a thermonuclear runaway event on a WD in binary systems, in which the WD accretes hydrogen-rich matter from the companion star. When the accreted matter reaches a critical value ($M_{\rm ig}$, see Fig.2), hydrogen at the bottom of the WD envelope ignites to trigger a shell flash. The decay phase of novae can be followed by a sequence of steady state solutions (Kato & Hachisu 1994). Using the same method and numerical techniques as in Kato & Hachisu (1994), Hachisu & Kato (2006, 2010) have followed evolutions of novae by connecting steady state solutions along the decreasing envelope mass sequence. The mass of the hydrogen-rich envelope is decreasing due to wind mass-loss and nuclear burning. They solved a set of equations, consisting of the continuity, equation of motion, radiative diffusion, and conservation of energy, from the bottom of the hydrogen-rich envelope through the photosphere assuming spherical symmetry. Winds are accelerated deep inside the photosphere so that they are called "optically thick winds." Hachisu & Kato (2006) have presented a unified model for IR, optical, UV, and supersoft X-ray light curves of the decay phase of classical novae. The optical and IR luminosity are reproduced by free-free emission from optically thin plasma. This free-free emission flux at the frequency ν is estimated from Equation (9) of Hachisu & Kato (2006), i.e.,

$$F_\nu \propto \frac{\dot{M}_{\rm wind}^2}{v_{\rm ph}^2 R_{\rm ph}}, \qquad (1)$$

where $\dot{M}_{\rm wind}$ is the wind mass-loss rate, $v_{\rm ph}$ the wind velocity at the photosphere, and $R_{\rm ph}$

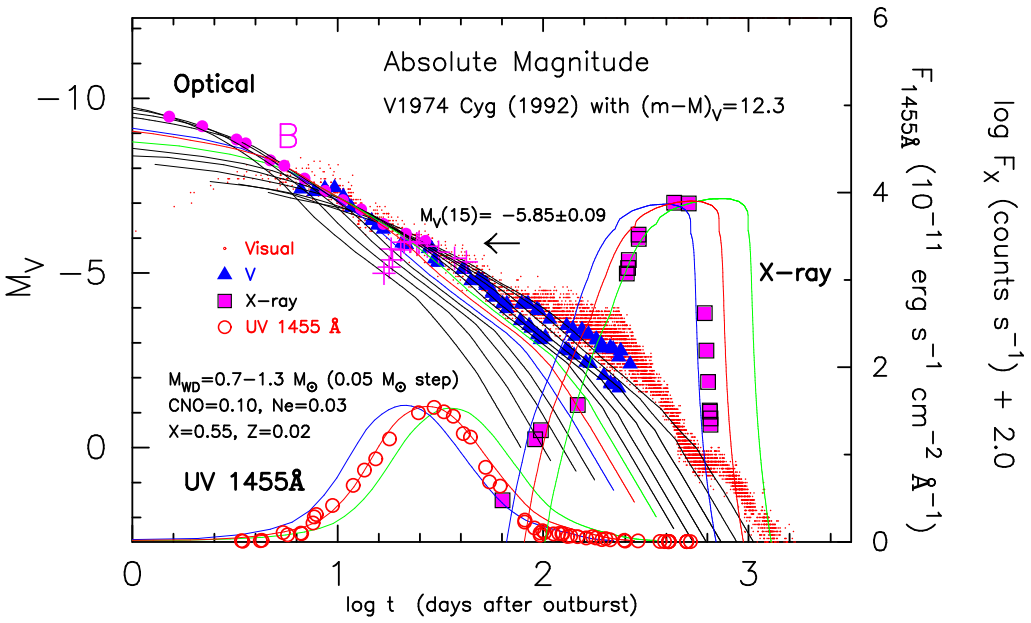

Fig. 7. Same as Fig.6 but for absolute magnitudes and real timescales (taken from Hachisu & Kato 2010). We have calibrated the free-free model light curves by a distance modulus of $(m - M)_V = 12.3$ for V1974 Cyg. The positions at point B in Fig.6 are indicated by a magenta filled circle. We also show the magnitude, $M_V(15)$, at 15 days after the optical maximum by a magenta cross. Their average value of $M_V(15) = -5.85 \pm 0.09$ is also indicated in the figure for 0.9–1.15 $M_\odot$ WDs. Model UV and supersoft X-ray light curves are omitted to simplify the figure except three WD masses (blue solid line for 1.1, red solid line for 1.05, and green solid line for 1.0 $M_\odot$).

the photospheric radius, all of which are taken from the wind solutions. Assuming a blackbody spectrum with the photospheric temperature of $T_{\rm ph}$, they have calculated the UV 1455 Å light curve for a narrow energy band of 1445–1465 Å (Cassatella et al. 2002) and the soft X-ray light curve for a range of 0.2–2.0 keV. The light curves of their optically thick wind model are parameterized by the WD mass ($M_{\rm WD}$), chemical composition of the WD envelope (X, Y, $X_{\rm CNO}$, $X_{\rm Ne}$, and Z), and envelope mass ($M_{\rm env,0}$) at the time of the outburst. Here X is the hydrogen, Y the helium, $X_{\rm CNO}$ the carbon-nitrogen-oxygen, $X_{\rm Ne}$ the neon, and Z the metallicity content of the envelope. The decay timescale of a light curve depends mainly on the WD mass and weakly on the chemical composition, whereas the maximum brightness of a light curve depends strongly on the initial envelope mass, $M_{\rm env,0}$. Figure 6 shows their free-free emission model light curves calculated from Equation (1), i.e.,

$$m_{\rm ff} = -2.5 \log \left[\frac{\dot{M}^2_{\rm wind}}{v^2_{\rm ph} R_{\rm ph}} \right]^{\{M_{\rm WD}\}}_{(t/f_{\rm s})} + \text{const.}, \qquad (2)$$

for various WD masses, from $M_{\rm WD} = 0.7$ to 1.3 $M_\odot$ by step of 0.05 $M_\odot$. The subscript $(t/f_{\rm s})$ explicitly expresses that this is a function of time while the superscript $\{M_{\rm WD}\}$ indicates a model parameter of WD mass. This shows that these model light curves are homologous and their shapes are almost overlapped with each other when they are properly squeezed or stretched along time (squeezed by a factor $f_{\rm s}$).

When we squeeze the model light curves by a factor of $f_{\rm s}$ in the time direction ($t' = t/f_{\rm s}$ and $\nu' = f_{\rm s}\nu$), the flux is also changed as $F'_{\nu'} = f_{\rm s} F_\nu$ because

$$\frac{d}{dt'} = f_{\rm s} \frac{d}{dt}. \qquad (3)$$

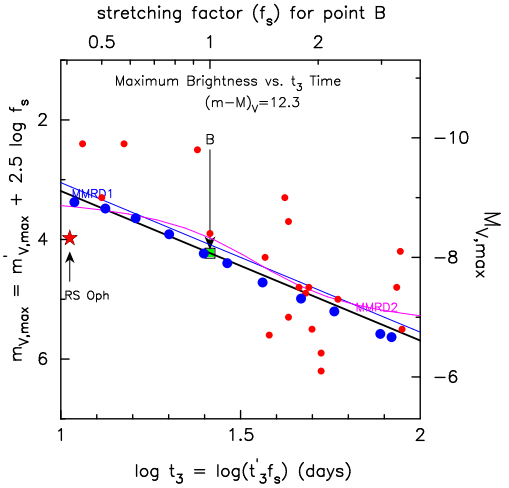

Fig. 8. The maximum magnitude–rate of decline (MMRD) relation against t_3 time. Point B represents the peak brightness of V1974 Cyg in Fig.7. The black solid line passing through B is corresponding to an MMRD relation of our model. Blue filled circles correspond to absolute magnitude of point B in Fig.7 from 1.25 to 0.75 $M_\odot$ by 0.05 $M_\odot$ step. The absolute magnitude $M_{V,\max}$ at maximum is obtained from calibration with V1974 Cyg of the distance modulus $(m - M)_V = 12.3$. Red filled star mark represent the recurrent nova RS Oph. Two well-known MMRD relations are added: Kaler-Schmidt's law (Schmidt 1957) labeled "MMRD1" (blue solid lines), and Della Valle & Livio's (1995) law labeled "MMRD2" (magenta solid lines). Red filled circles denote MMRD points for individual Galactic novae taken from Table 5 of Downes & Duerbeck (2000).

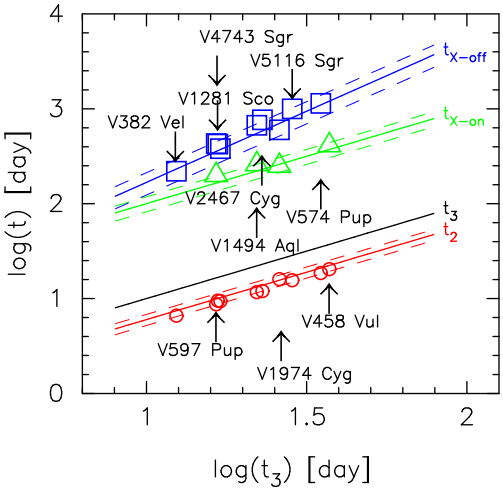

Fig. 9. Supersoft X-ray on/off and "intrinsic" t_2 time against "intrinsic" t_3 time taken from Hachisu & Kato (2010). We plot 10 novae, i.e., V1974 Cyg 1992, V382 Vel 1999, V1494 Aql 1999#2, V4743 Sgr 2002, V574 Pup 2004, V5116 Sgr 2005, V1281 Sco 2007, V2467 Cyg 2007, V458 Vul 2007, and V597 Pup 2007#1.

For free-free emission, we have $F'_{\nu'} = F'_\nu$ =const and then have the following relation and can shift the model light curves in the vertical direction as

$$m'_V = m_V - 2.5 \log f_s. \quad (4)$$

Then the absolute V magnitudes can be written as

$$\begin{aligned} M_V &= m_V - (m - M)_{V,\mathrm{V1974Cyg}} \\ &= m'_V + 2.5 \log f_s - (m - M)_{V,\mathrm{V1974Cyg}}. \end{aligned} \quad (5)$$

Here, m'_V is the apparent V magnitude of V1974 Cyg and we adopt the distance of d = 1.8 kpc (Chochol et al. 1993) and the absorption of $A_V = 1.0$, so $(m - M)_{V,\mathrm{V1974\ Cyg}} = 12.3$. The absolute magnitude of each light curve is recovered in Figure 7 for various WD masses. The Maximum Magnitude versus Rate of Decline (MMRD) relation is often used to estimate the distance to novae. In Figure 8, we show the result of Figure 7. This clearly demonstrates a trend that a more massive WD has a brighter maximum magnitude (smaller $M_{V,\max}$) and a faster decline rate (smaller t_3 time). The relation between t_3 (or t_2) and $M_{V,\max}$ for novae is called "the Maximum Magnitude–Rate of Decline" (MMRD) relation. Here t_3 (t_2) time is defined by 3-mag (2-mag) decay time from maximum in units of day. See Hachisu & Kato (2010) for more details. Nova light curves follow a universal decline law, that is, several timescales of t_2, t_3, $t_{\rm break}$, and $t_{\rm wind}$ could be related with each other in a linear regime. Here $t_{\rm break}$ is the time at a break of our model light curve and $t_{\rm wind}$ is the time at which the optically thick wind stops. Only the timescale of $t_{\rm H-burning}$ (time at the end of H-burning) is not a linear but a non-linear regime. So we can derive relations among $t_{\rm H-burning}$, $t_{\rm wind}$, and t_3 (or t_2). Once we determine t_3 (or t_2) of individual novae

from observations, we may theoretically estimate the duration of a luminous supersoft X-ray phase by using

$$t_{\rm X-on} \approx t_{\rm wind} = (2.6 \pm 0.4)\, t_{\rm break}, \quad (6)$$

$$t_{\rm X-off} \approx t_{\rm H-burning} = (0.71 \pm 0.1)\, (t_{\rm break})^{1.5}, \quad (7)$$

$$t_{\rm X-off} \approx t_{\rm H-burning} = (0.17 \pm 0.023)\, (t_{\rm wind})^{1.5}, \quad (8)$$

$$\frac{t_3}{t_{\rm break}} = \frac{t_3/f_{\rm s}}{t_{\rm break}/f_{\rm s}} = 0.26 \pm 0.04, \quad (9)$$

and

$$t_2 = (0.6 \pm 0.08)\, t_3. \quad (10)$$

It should be noted that the proportionality of $t_{\rm wind}$ to $t_{\rm break}$, i.e., $t_{\rm wind}/t_{\rm break} \approx 2.6$, is a direct result of our scaling law (the universal decline law), because both $t_{\rm break}$ and $t_{\rm wind}$ are during the optically thick wind phase which is the subject of universal decline law. Then the $t_{\rm wind}$ is directly proportional to $t_{\rm break}$. On the other hand, the turnoff time of hydrogen shell burning, $t_{\rm H-burning}$, is not proportional to $t_{\rm break}$ or $t_{\rm wind}$, because the duration of static hydrogen shell burning phase depends on hydrogen content X (amount of fuel) of the envelope and WD mass (temperature) in a different way from the optically thick wind phase, in which the decay rate is determined mainly by wind mass-loss not by hydrogen burning rate. Therefore, Equations (7) and (8) are empirical laws obtained numerically, the power of which is not 1.0 but approximately 1.5. It is very useful if we can predict $t_{\rm X-on}$ ($\approx t_{\rm wind}$) and $t_{\rm X-off}$ ($\approx t_{\rm H-burning}$) from t_3 time, because t_3 is popular and widely used to define the nova speed class, that is,

$$t_{\rm X-on} \approx t_{\rm wind} = (10.0 \pm 1.8)\, t_3, \quad (11)$$

$$t_{\rm X-off} \approx t_{\rm H-burning} = (5.3 \pm 1.4)\, (t_3)^{1.5}. \quad (12)$$

We have examined 10 classical novae and showed them in Figure 9, i.e., V1974 Cyg, V382 Vel, V4743 Sgr, V1281 Sco, V597 Pup, V1494 Aql, V2467 Cyg, V5116 Sgr, V574 Pup, and V458 Vul. In all 10 novae, a supersoft X-ray phase was detected, so we can check whether or not our prediction formulae of a supersoft X-ray phase work on these novae. They are reasonably consistent with our prediction formulae.

4. Discussion

CHRISTIAN KNIGGE: A question to all nova modelers. Really there are observational indications that the WD masses in CVs are greater than in isolated WDs (Zorotovic, Schreiber, & Gansicke 2011). But all nova models suggest that the WD mass slowly decreases – so what's wrong?

IZUMI HACHISU: In low mass WDs ($\lesssim 0.6\ M_\odot$) shell flashes evolve very slowly ($\gtrsim 10$ yr), so it may not look like a classical nova. Enrichment of heavy elements in classical novae suggest that the WD core material was dredged up, indicating an erosion of the WD core.

References

Alcock, C. et al. 1996, MNRAS, 280, L49
Cassatella, A., Altamore, A., & González-Riestra, R. 2002, A&A, 384, 1023
Chochol, D., et al. 1993, A&A, 277, 103
Della Valle, M., & Livio, M. 1995, ApJ, 452, 704
Downes, R. A., & Duerbeck, H. W. 2000, AJ, 120, 2007
Hachisu, I., & Kato, M. 2001, ApJ, 558, 323
Hachisu, I., & Kato, M. 2003a, ApJ, 590, 445
Hachisu, I., & Kato, M. 2003b, ApJ, 598, 527
Hachisu, I., & Kato, M. 2006, ApJS, 167, 59
Hachisu, I., & Kato, M. 2010, ApJ, 709, 680
Hachisu, I., Kato, M., & Nomoto, K. 1996, ApJ, 470, L97
Kato, M., & Hachisu, I. 1994, ApJ, 437, 802
Krautter, J., et al. 1996, ApJ, .456, 788
Nomoto, K. 1982, ApJ, 253, 798
Nomoto, K., Saio, H., Kato, M., & Hachisu, I. 2007, ApJ, 663, 1269
Reinsch, K., van Teeseling, A., King, A. R., & Beuermann, K. 2000, A&A, 354, L37
Schmidt, Th. 1957, Z. Astrophys., 41, 181
Šimon, V., & Mattei, J. A. 1999, A&AS, 139, 75